Proceedings of the 4th International Conference on Applied Physics and Mathematical Modeling
DOI: 10.54254/2753-8818/2026.37947

Sensitivity of e^N Transition Prediction to the Empirical N-Factor: A Parametric XFOIL Study on a Thin Symmetric Airfoil

Letong Zheng

Woodside Priory School, Portola Valley, USA
zhengletong642@gmail.com

Abstract. Boundary-layer transition strongly influences surface skin friction and is therefore important in laminar-flow aerodynamic design. This study combines a review of the classical transition pathway with a parametric sensitivity analysis of the semi-empirical e^N method. The review traces transition from Tollmien–Schlichting wave amplification through secondary instability and Λ-vortex formation to turbulent breakdown, while highlighting the receptivity limitation that prevents N_{crit} from being determined purely from linear stability theory. Transition prediction is then performed using XFOIL 6.99 with a NACA 0008 airfoil as a thin, near-zero-pressure-gradient proxy. Three single-variable studies examine chord Reynolds number. (10^5-10^7), N_{crit} (4–13), and angle of attack (-4° to +4°). Increasing Reynolds number moves the predicted transition upstream from x_{tr}/c=1.000 to 0.344. At Re=10^6, increasing N_{crit} from 4 to 13 shifts transition downstream from 0.556 to 0.943. Varying incidence moves transition in opposite directions on the two surfaces, spanning almost the entire chord within ±4°. These results show that e^N-based transition prediction is highly sensitive to Reynolds number, the empirical N_{crit} and even weak pressure gradients, emphasising the uncertainty introduced by unmodelled receptivity and geometric approximation.

Keywords: Boundary-layer transition, e^N method, N_{crit}, XFOIL, Tollmien–Schlichting waves

1. Introduction

The transition of boundary layer from a laminar to turbulent flow is one of the classical problems of fluid dynamics. This is not only a physical problem but also involves the cost of its practice, as turbulent skin friction is substantially higher than laminar skin friction, so the exact location where this transition occurs largely determines the magnitude of the energy lost to friction. On an aircraft wing, this transition location directly affects fuel consumption and emissions. In other words, being able to predict or delay this transition is a practical engineering goal, which is also the central aim of laminar-flow-control design.

For a flat-plate boundary layer at zero pressure gradient and low free-stream turbulence, the classical transition pathway has been well established. The Small disturbances are amplified as Tollmien-Schlichting waves; once their amplitude reaches a certain per cent of the free-stream

© 2026 The Authors. This is an open access article distributed under the terms of the Creative Commons Attribution License 4.0 (https://creativecommons.org/licenses/by/4.0/).

DOI: 10.54254/2753-8818/2026.37947

velocity, the secondary instabilities generate three-dimensional Λ-vortices that break down into turbulence. This is a typical turning path under the conditions of low current turbulence and zero pressure gradient; under the condition of high current turbulence, the T-S wave stage will no longer play a dominant role, at which time the transient strip growth and its secondary instability may occupy a dominant position. According to Kachanov, the transition is predicted by using the semi-empirical e^N method, which integrates the linear growth rate of these T-S waves and assumes the transition occurs when the amplification factor N reaches the critical value N_{crit} [1]. However, this method has a fundamental limitation: linear stability theory can only determine the growth rate of the disturbance, but not the initial amplitude from which it grows. As a result, cap N sub crit cannot be derived from first principles and must be calibrated empirically for each environment. This article aims to evaluate how this empirical choice affects the predicted transition location and the uncertainty it introduces.

2. The classical transition pathway

The natural transformation process of the flat boundary layer under the zero pressure gradient includes several stages that have been fully studied. Kachanov summarizes the transformation of the boundary layer into two major categories [1]. This article will discuss the first category: that is, how the instability of the boundary layer itself is amplified and interacts, which eventually leads to the collapse of the laminar flow structure. This section will review this evolutionary path in two parts, covering the linear growth of disturbances and the process of nonlinear collapse.

2.1. Linear stage: Tollmien–Schlichting waves

Laminar flow is a smooth and ordered flow with momentum exchanged between layers only through molecular diffusion. External disturbances, such as surface roughness, are governed by the Reynolds number, which reflects the balance relationship between the destabilising and stabilising effects acting on it. When the Reynolds number is below a critical value, viscous dissipation outweighs the energy disturbance it can extract from the mean shear, leading to the decay of the disturbance.

Meanwhile, when it is above the critical value, the linear stability equation allows a band of frequencies with a positive growth rate, which are amplified along the flow as Tollmien-Schlichting waves. During the process of amplification, when the wave's amplitude is below a certain per cent of the free stream velocity, the disturbance mode grows independently and obeys the linear superposition principle, and the laminar flow remains ordered despite the distortion.

2.2. Nonlinear stage: secondary instability and breakdown

Once the disturbance amplitude exceeds a certain per cent of the average flow rate, the superposition principle is no longer applicable. Energy exchange occurs between waves of different frequencies, and new disturbances that do not exist in the original spectrum are produced. The most significant consequence is the loss of two-dimensional characteristics of flow, and three-dimensional vortex structures appear in TS waves.

These vortex structures are Λ-shaped and arranged in one of two patterns: arranged along the flow in the K-type evolution path, or staggered in the subharmonic H-type evolution path. At the tips of these Λ-shaped vortices, the local velocity profile undergoes severe distortion and forms a strong internal shear layer [2, 3]. Because this speed profile with an inflection point is itself unstable, these high shear layers will quickly roll up and produce high-frequency oscillations. These local

DOI: 10.54254/2753-8818/2026.37947

disturbance eruptions will evolve into turbulence spots; as they are transported downstream, the turbulence spots continue to grow and merge with each other, eventually covering the entire surface, transforming the boundary layer into a completely turbulent state.

3. Limitations of the classical pathway

Although classical transition pathways describe the transition process well, they are built on some key assumptions. Here are two limitations that matter in this article and will be discussed in the parametric study in Section 6.

3.1. Initial disturbance energy and receptivity

The rate at which a disturbance grows can be predicted using linear stability theory, but the amplitude of that disturbance at its inception cannot be found using linear stability theory. That initial amplitude is set by receptivity — the process by which external disturbances such as free-stream turbulence, acoustic noise, and surface roughness enter the boundary layer and excite T–S waves [2]. Since receptivity will depend on the disturbance environment, the initial amplitude is unknown from the stability equations, which results in the starting point of the whole amplification being undetermined by the theory.

3.2. The empirical nature of the e^N method

The e^N method directly integrated the spatial growth rate of the most amplified T-S wave to obtain the amplification factor N, assuming that the transition happens when N reaches the critical value N_{crit}. Since this paper didn't model the initial amplitude and disturbance environment, N_{crit} is not a physical constant but a calibration parameter that a quiet facility corresponds to a high N_{crit} and a noisy one to a lower value, which may require this paper to empirically determine its value.

4. Methodology

4.1. The e^N method and the XFOIL implementation

The e^N method quantifies the linear growth of the disturbance by amplification factor N; N, the amplification factor, is defined as $N(x) = \ln[A(x)/A_0]$, where A_0 is the amplitude of that disturbance at the neutral point x_0, which is the streamwise station when the frequency becomes unstable. In this definition, the neutral point is a mathematical reference fixed by the stability equations, not the location at which the disturbance physically originates, and A_0 is correspondingly not the amplitude imposed by the external disturbance environment. Equally, N can also be expressed as the integral of the local space growth rate along the boundary layer, so the disturbance with the magnification of e^N corresponds to the N value. It is usually assumed that the transition occurs at the position where N reaches the selected critical value. N_{crit} for the first time. Since N_{crit} covers all unmodeled and environmental effects discussed in Section 3, it is regarded as a variable input parameter rather than a fixed constant.

The entire experimental computation is conducted in the software called XFOIL 6.99, a freely available panel-method code that could couple an inviscid panel solution and integral boundary-layer formation, and built in a e^N transition predictor [4, 5]. In the experiment, XFOIL reports the transition location on the upper and lower surfaces using the chordwise position N_{crit}, which is the major output variable in this study [6]. Moreover, XFOIL operates on airfoils rather than on an

DOI: 10.54254/2753-8818/2026.37947

isolated flat plate. This paper utilises a NACA 0008 symmetric airfoil at zero angle of attack to approximate the zero-pressure-gradient flat plate [7]. Such an approximation requires justification, as it is a potential source of error. The symmetric airfoil does not generate lift at zero angle of attack; therefore, its upper and lower surfaces are exactly the same, and the predicted transition location is also the same. However, the limited thickness and surface curvature of the wing will still produce a weak flow pressure gradient that the real flat plate does not have: the airflow accelerates at the front of the wing and slows down when it flows to the rear edge. The reason why the thin wing type (thickness of 8%) is deliberately selected is to reduce this residual pressure gradient, but it cannot be completely eliminated, which also constitutes the limitation of the approximate method. Therefore, the results obtained should be regarded as the change trend of thin, near-zero pressure gradient wings, rather than the exact value of the flat plate [8-10].

4.2. Case matrix

A total of three parameter scans were carried out, changing one variable each time, while keeping other parameters unchanged. Unless otherwise stated, the geometry (NACA 0008), Mach number (0, i.e. incompressible flow) and the number of face elements (160, automatically divided by XFOIL) under all working conditions are consistent. The Reynolds number is defined by the wing chord length c, and the transition location is expressed as the position x_{tr}/c along the chord direction.

Study A — Effect of Reynolds Number for the Transition Process. The N_{crit} value is fixed at the conventional value of 9, and the angle of attack at 0°, and the chord-based Reynolds number was chosen across Re = 1×10^5, 5×10^5, 1×10^6, 3×10^6, 5×10^6, and $1\times10^7$to show the trend of the transition location as Reynolds number increases.

Study B —Effect of the Critical N-factor. With Re fixed at 1×10^6 and the angle of attack at 0°, N_{crit} was varied across 4, 7, 9, 11, and 13, spanning conditions from a relatively noisy free stream (low N_{crit}) to a very quiet one (high N_{crit}) to the relationship between the N_{crit} value with the transition location.

Study C —Effect of Airfoil Pressure Distribution With Re fixed at 1×10^6 and N_{crit} at 9, a streamwise pressure gradient was introduced by varying the angle of attack across α = −4°, −2°, 0°, +2°, and +4°. Here, the two surfaces are treated separately because the transition no longer occurs in the same position on the two surfaces. Unlike studies A and B, the lift coefficient in this scan is deliberately set to non-zero, because the non-zero angle of incidence is the way to apply the pressure gradient.

5. Results

5.1. Effects of reynold number

Study A shows how the predicted transition location varied with the change of the chord-based Reynolds number, and the N_{crit} is always held at 9 in this part. The results are listed in Table 1 and plotted in Figure 1, demonstrating that as the Reynolds number rises, the transition point moves monotonically upstream—from x_{tr}/c =1.000 at Re = 1×10^5, to x_{tr}/c = 0.953 at Re = 5×10^5, 0.854 at 1×10^6, 0.600 at 3×10^6, 0.483 at 5×10^6, and 0.344 at 1×10^7. Over the two orders of magnitude in Reynolds number, the predicted location shifts roughly about two-thirds of the chord.

DOI: 10.54254/2753-8818/2026.37947

Table 1. Effect of Reynolds number on the predicted transition location

Reynold Number	N_{crit}	x_{tr}/c
1×10^5	9	1.000
5×10^5	9	0.953
1×10^6	9	0.854
3×10^6	9	0.600
5×10^6	9	0.483
1×10^7	9	0.344

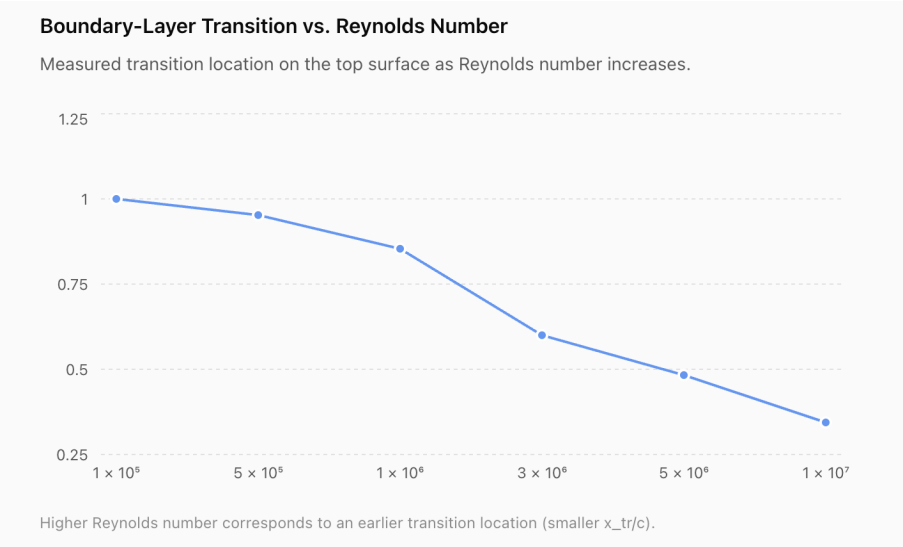


Figure 1. Predicted boundary-layer transition location at different reynolds numbers (picture credit: original)

Physically, the higher Reynolds number enhances the inertial effect of driving the growth of disturbances, so that the amplification of T-S waves (Tollmien-Schlichting waves) is more rapid, and the amplification factor can reach N_{crit} in a shorter flow distance. In the case of the lowest Reynolds number, the disturbance growth is too weak to accumulate enough magnifications within the chord length range, which is the reason why the transition is completely suppressed.

5.2. Effect of the critical N-factor

Study B examined the sensitivity of the predicted transition location to the critical N-factor, with the Reynolds number held fixed at 1×10^6 in this part. The results are listed in Table 2 and plotted in Figure 2. Transition moves monotonically downstream as N_{crit} increases: from $x_{tr}/c = 0.556$ at $N_{\text{crit}} = 4$, to 0.765 at 7, 0.854 at 9, 0.909 at 11, and 0.943 at 13.

DOI: 10.54254/2753-8818/2026.37947

Table 2. Effect of the critical N-Factor on the predicted transition location

Reynold Number	N_{crit}	x_{tr}/c
1×10⁶	4	0.556
1×10⁶	7	0.765
1×10⁶	9	0.854
1×10⁶	11	0.909
1×10⁶	13	0.943

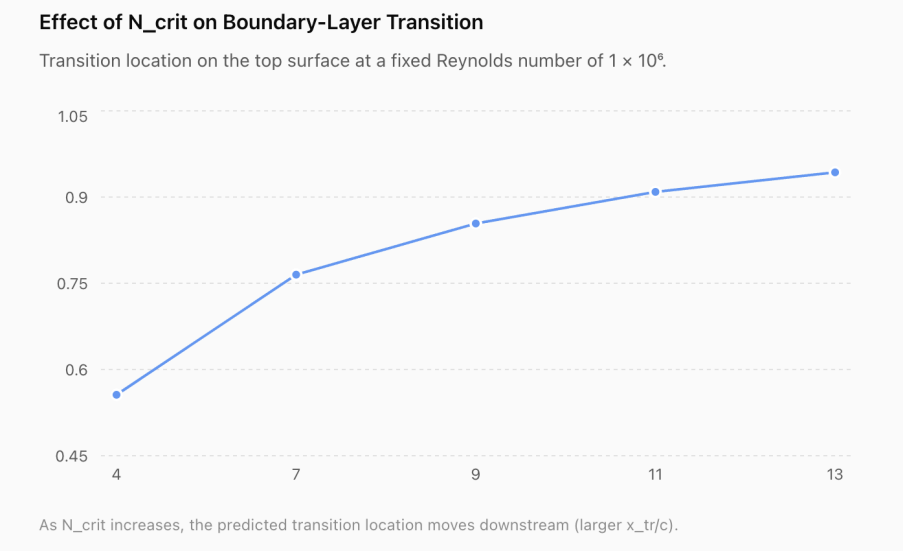


Figure 2. Predicted boundary-layer transition location at different ncrit values (picture credit: original)

The key observation is the magnitude of this change - the predicted transition location has moved nearly 40% of the chord length (from 56% to 94%). From a physical point of view, a larger N_{crit} value means a quieter inflow environment; in this environment, the disturbance must be amplified by a larger number of times to trigger the transition, thus causing the transition point to be downstream in the flow. The result confirms that the predicted transition location is highly sensitive to this parameter; as described in Section 3, this parameter cannot be determined by theory, but must be set based on experience.

5.3. Effect of airfoil pressure distribution

Study C examines how the streamwise pressure gradient would affect the transition point, which is imposed by varying the angle of attack from −4°, 2 °, 0°, +2° to +4° when the Reynold number is fixed at 1*10^6, and N_{crit} is at 9. Since the incident angle is no longer just 0, the transition locations on the top and bottom plates are different, as they are plotted in Figure 3 and reported in Table 3.

DOI: 10.54254/2753-8818/2026.37947

Table 3. Effect of angle of attack on the predicted transition locations of the upper and lower surfaces

Angle α	Top x_{tr}/c	Bottom x_{tr}/c
−4°	1.000	0.061
−2°	0.986	0.476
0°	0.854	0.854
+2°	0.476	0.986
+4°	0.061	1.000

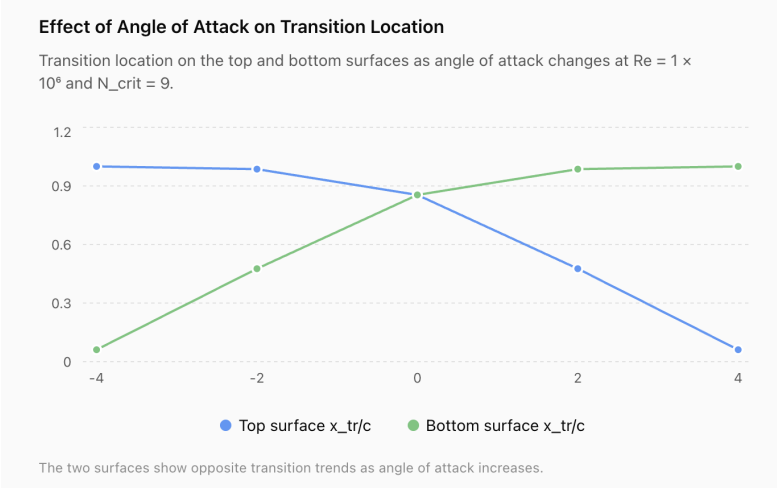


Figure 3. Variation of upper- and lower-surface transition locations with angle of attack (picture credit: original)

The transition location shows symmetry about zero incidence with the change of the angle of attack: when α = 0°, both surfaces shift at x_{tr}/c = 0.854; however, with an increase in the angle of attack, the transition location of the suction surface moves sharply to the front edge of the wing, and the pressure transition of the force surface (in the pressure gradient zone) is delayed. When the angle of attack reaches 4°, the pressure surface maintains the laminar flow state until the rear edge. Therefore, only in the range of ±4° angle of attack, the predicted transition location spans almost the entire chord length, indicating that the influence of the pressure gradient is at least comparable to the Reynolds number N_{crit}. Given that only the working conditions of α = 0° correspond to the true zero-pressure gradient plate flow, this high sensitivity confirms that even the weak residual pressure gradient generated by the curvature of the wing type itself is enough to significantly change the predicted transition location.

6. Discussion

6.1. Connection to the receptivity limitation

As discussed in 5.2, the predicted transition location moved from x_{tr}/c = 0.556 at N_{crit} = 4 to 0.943 at N_{crit} = 13, which is nearly 40 per cent of the entire chord. This sensitivity becomes a direct numerical expression of the receptivity present in section 3. As this paper discussed in the previous

DOI: 10.54254/2753-8818/2026.37947

section, the Linear Stability Theory determines the rate of growth of a disturbance but not the initial amplitude that the disturbance starts as; nevertheless, this initial amplitude is fixed by the receptivity–the process that the external environment seeds the disturbance. Because e^N never models this stage, everything that determines the initial amplitude is folded into N_{crit}.

Therefore, the closure of this logical chain can only depend on experience: the level of external disturbance determines the receptivity, which in turn determines the initial amplitude of the T-S wave, and then determines the amplification required for fluid collapse. Research B examines the sensitivity of the final prediction results to the last link in the chain. The significant changes observed from this are not an artifact of numerical calculation, but a quantification of the degree of prediction uncertainty introduced by the "unmodeled receptivity". In this sense, parametric results and theoretical limitations both describe the same limitation from two different perspectives.

6.2. Limitations of this study

These results are constrained by a number of limitations. First of all, the e^N method is based on the cumulative linear amplification of disturbance, so it only simulates the linear growth stage in the transition process. The method stops calculating when the N value reaches the critical value. N_{crit} and the ensuing nonlinear collapse process cannot be described. Therefore, the applicability of this method will be reduced accordingly when the linear T-S mechanism, such as strong nonlinear flow state, bypass transition and high flow turbulence, does not dominate the transfer path. Secondly, the XFOIL is a two-dimensional, viscous–inviscid interaction code rather than a full simulation for the Navi-Stocks function, so it cannot capture three-dimensional flows, and the results should be read as a trend rather than an exact value. Lastly, the flat-plate condition is approximated by a thin symmetry airfoil at zero incidence. As shown in Study C, the transition process is very sensitive to even a weak pressure gradient, and the finite curvature of the wing will produce a tiny residual gradient that does not exist in a real flat plate.

Eventually, the transition location reported here should therefore be understood as applying to a thin, near-zero-pressure-gradient section; the conclusion of this study is mainly based on various changing trends - that is, the monotonous response with the change of Reynolds number (Re), the high sensitivity to the critical disturbance amplification factor N_{crit} and pressure, the opposite effect of the gradient - and these trends are robust for the above approximate treatment.

7. Conclusion

This paper combines a review of the traditional transition pathway in a flat-plate boundary layer with a parametric study of the factors that influence the transition location through the e^N prediction method using XFOIL.

The review establishes the classical transition path under the condition of low incoming turbulence and zero pressure gradient: the linear stage of small disturbance evolves into Tollmien-Schlichting waves and is amplified; when its amplitude reaches a percentage of the incoming velocity, the secondary instability produces a Λ-type vortex, and then breaks down to form turbulence. In engineering practice, this path is usually predicted by the semi-empirical e^N method, but the critical amplification factor N_{crit} in this method cannot be derived from theory and must be calibrated according to the specific environment.

Furthermore, the parametric study examines how the predicted transition location responds to the three factors. In Study A, with the increase of the Reynolds number, the transition position moves upstream. Within the range of two orders of magnitude, its movement distance is about two-thirds of

DOI: 10.54254/2753-8818/2026.37947

the chord length; and with the increase of the critical value of N_{crit}, the transition position moves downstream. When N_{crit} changes from 4 to 13 in Study B, its movement span is close to 40% of the chord length; this large displacement comes from modelling selection and inflow environment rather than fluid physical properties, which directly reflects the restriction of the receptivity that the method does not include in the initial condition. Finally, in Study C, imposing a pressure gradient through the angle of attack moves transition in opposite directions on the two surfaces: over only ±4° of incidence, the transition location spans almost the entire chord length. These results show that the predicted transition position depends not only on the Reynolds number, but also strongly on the empirical parameter. N_{crit} and pressure gradient.

As the e^N method could only describe the transition within the linear stage, this paper could extend it to the stage that it cannot capture; for example, the bypass transition under high-free-stream turbulence. Comparing these against the classical transition pathway would clarify why a single method could not predict the transition in all geometries.

Furthermore, the most direct problem is the approximation of the flat panel. Here, a symmetrical wing with zero angle of attack is used to approximate the zero pressure gradient plate, but research C shows that even with a mild pressure gradient, the transition is very sensitive, and the curvature of the wing type itself will produce a small residual gradient that the real plate will not have. Future development for this study may involve using code or geometry to represent the real flare plate in order to minimise the approximation impact on the real behaviour.

References

[1] Kachanov, Y. S. (1994). Physical mechanisms of laminar-boundary-layer transition. *Annual Review of Fluid Mechanics, 26*, 411–482. https://doi.org/10.1146/annurev.fl.26.010194.002211

[2] Saric, W. S., Reed, H. L., & Kerschen, E. J. (2002). Boundary-layer receptivity to freestream disturbances. *Annual Review of Fluid Mechanics, 34*, 291–319. https://doi.org/10.1146/annurev.fluid.34.082701.161921

[3] Herbert, T. (1988). Secondary instability of boundary layers. *Annual Review of Fluid Mechanics, 20*, 487–526. https://doi.org/10.1146/annurev.fl.20.010188.002415

[4] Maughmer, M. D., Axten, C. J., & Metkowski, L. P. (2023). Experimental results for a low-Reynolds-number airfoil in a low-turbulence wind tunnel. *Journal of Aircraft, 60*(6), 1739–1745. https://doi.org/10.2514/1.C036705

[5] Placidi, M., Ashworth, R., Atkin, C. J., & Rolston, S. (2023). Effect of environmental disturbances on crossflow instability. *Experiments in Fluids, 64*, 37. https://doi.org/10.1007/s00348-023-03579-x

[6] Blanco, D. C. P., Hanifi, A., Henningson, D. S., & Cavalieri, A. V. G. (2024). Linear and nonlinear receptivity mechanisms in boundary layers subject to free-stream turbulence. *Journal of Fluid Mechanics, 979*, A15. https://doi.org/10.1017/jfm.2023.1035

[7] Römer, T. M., Kloker, M. J., Rist, U., & Wenzel, C. (2024). Experimental investigation of boundary-layer streaks induced by grid-generated free-stream turbulence in a water channel. *Experiments in Fluids, 65*, 187. https://doi.org/10.1007/s00348-024-03917-7

[8] Toppings, C. E., & Yarusevych, S. (2024). Laminar separation bubble formation and bursting on a finite wing. *Journal of Fluid Mechanics, 986*, A26. https://doi.org/10.1017/jfm.2024.321

[9] Toppings, C. E., & Yarusevych, S. (2025). Low-Reynolds-number aerofoil boundary layer transition in large-scale free stream turbulence. *Journal of Fluid Mechanics, 1021*, A46. https://doi.org/10.1017/jfm.2025.10747

[10] Ren, X., Ghopa, W. A. W., Rasani, M. R., & Harun, Z. (2026). Research progress on laminar separation bubble dynamics and aerodynamic optimization of low-Reynolds-number airfoils. *Frontiers in Mechanical Engineering, 12*, 1850561. https://doi.org/10.3389/fmech.2026.1850561